

Characteristics of Anomalous Transport and Losses of Energetic Ions Caused by Alfvénic Modes in LHD Plasmas

M. Isobe 1,2), K. Ogawa 3), K. Toi 1,3), M. Osakabe 1), K. Nagaoka 1), T. Tokuzawa 1,2),
S. Kobayashi 4), D.A. Spong 5), D.S. Darrow 6) and LHD experiment group 1)

1) National Institute for Fusion Science, Toki 509-5292 Japan

2) Department of Fusion Science, The Graduate University for Advanced Studies, Toki 509-5292 Japan

3) Department of Energy Science and Engineering, Nagoya University, Nagoya 464-8603 Japan

4) Institute for Advanced Energy, Kyoto University, Uji 611-0011 Japan

5) Oak Ridge National Laboratory, Oak Ridge, TN 37831 USA

6) Princeton Plasma Physics Laboratory, Princeton, NJ 08543-0451 USA

E-mail contact of main author: isobe@nifs.ac.jp

Abstract. Anomalous transport and losses of energetic ions caused by Alfvénic modes in neutral beam-heated Large Helical Device (LHD) plasmas are studied with a scintillator-based lost fast-ion probe (SLIP) and a charge-exchanged neutral particle analyzer. Correlated with recurrent bursting toroidicity-induced Alfvén eigenmodes (TAEs), significant increases of energetic-ion losses are observed. Co-going transit energetic ions are responsible for destabilization of TAEs in LHD and are anomalously expelled through a diffusive-type loss mechanism. A particle simulation with a modeled perturbed magnetic field suggests that energetic-ion losses increase as the amplitude of the perturbed field increases. Experimentally measured pitch-angle distributions of escaping beam ions are reproduced by particle simulation.

1. Introduction

Good confinement of energetic ions in magnetically confined fusion plasmas is required in order to realize a fusion reactor, since fusion-born energetic alpha particles play an essential role as a primary heating source in future burning plasmas. With a burning plasma stage imminent, the physics of the interplay between energetic ions and energetic-ion-driven magnetohydrodynamic (MHD) instabilities such as toroidicity-induced Alfvén eigenmodes (TAEs) [1] and energetic-particle continuum modes (EPMs) [2] have become more important in recent years. This is because those MHD instabilities can potentially lead to the anomalous loss of energetic alpha particles, resulting in the loss of a self-ignited condition. Alfvénic modes have been regularly observed in tokamak plasmas with strong super-Alfvénic ion tails [3,4]. They have been also observed in heliotron/stellarator plasmas [5,6]. In these circumstances, the excitation/damping mechanisms of those instabilities and their effects on energetic-ion behavior are being investigated intensively in existing toroidal fusion devices [7-10]. In the Large Helical Device (LHD), the non-classical transport of co-going beam ions due to bursting TAEs has been so far recognized from the measurement of charge-exchanged (CX) fast neutrals [11]. For a better understanding of the effects of those instabilities on energetic-ion transport and/or loss in heliotron/stellarator plasmas, the energetic-particle diagnostic system on LHD has been extended in FY2008-2009. This work is devoted to the study of the impacts of energetic-ion-driven MHD instabilities on anomalous transport and consequent losses of energetic ions in LHD.

2. Experimental setup

2.1 Energetic ions in LHD

LHD is the world's largest superconducting magnetic confinement device, having a major radius R of 3.9 m and an average plasma minor radius a of ~ 0.6 m. The toroidal periods M and multipolarity l are 10 and 2, respectively [12]. The toroidal magnetic field strength can be increased up to 3 T. LHD is equipped with five high-energy neutral beam (NB) injectors [13]. Three of them are based on a negative-ion source, here called N-NBIs. Each N-NBI can provide high-energy beam ions in the tangential direction with injection energy E_b of 180 keV and port-through power of ~ 5 MW. Two of the N-NBIs are oriented in the counter-clockwise direction as seen from the top, and another has the opposite direction. Energetic beam ions injected by N-NBIs are super-Alfvénic in many cases.

2.2 Diagnostics

A comprehensive set of energetic-particle diagnostics is installed on LHD [14]. To reveal energetic-ion behaviors while energetic-ion-driven MHD instabilities are present, a CX E//B-type neutral particle analyzer (NPA) having a tangential line of sight and a scintillator-based lost-fast ion probe (SLIP) placed at the outboard side play important roles in this study. The former can provide time-resolved information on confined transit beam ions with a pitch-angle range ($\chi = \arccos(v_{\parallel}/v)$) less than 50 degrees in $R > R_{ax}$, while the latter is capable of detecting lost energetic ions outside of the plasma. The SLIP is classified as a magnetic spectrometer and provides both gyroradius centroid ρ_h , i.e.

the energy and pitch angle of escaping energetic ions reaching the SLIP simultaneously as a function of time. The SLIP is designed so as to detect escaping energetic ions having ρ_h from 2 cm to 23 cm and χ from 30 degrees to 80 degrees at the SLIP position. The intensity and distribution of scintillation light on the scintillator screen due to the impact of escaping energetic ions are measured with both an image-intensified fast CMOS camera and 16 photomultiplier tubes (PMTs). A detailed description of the SLIP is available in Ref. 15. Figure 1 depicts the arrangement of NBIs, SLIP at the outboard side and E//B-type NPA on LHD.

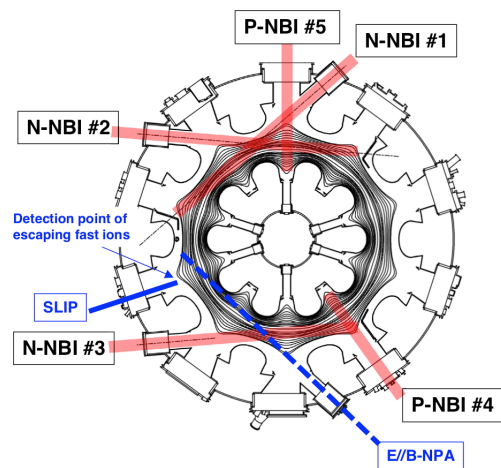


FIG.1. Arrangement of NBIs, SLIP placed at the outboard side and E//B-type NPA.

3. Experimental results

3.1 TAEs driven by energetic beam ions in LHD

TAEs are often destabilized in LHD when super-Alfvénic ions are present in high β plasmas. Figure 2 shows typical waveforms in the quasi-stationary phase of TAE discharge at R_{ax}/B_t of 3.6 m/0.6 T (CCW) when three N-NBs are tangentially injected. The volume-averaged plasma beta value $\langle \beta \rangle$ is relatively high, about 2%, and energetic-ion beta $\langle \beta_h \rangle$ is estimated to be about 1%, i.e., comparable to $\langle \beta \rangle$. The ratio of initial beam ion velocity to the Alfvén velocity v_{\parallel}/v_A is about 2. As can be seen in Fig. 2e), strong recurrent bursting magnetic fluctuations appear in the frequency range of 50~80 kHz. Analysis of the Mirnov coil array signal suggests that this mode has a structure of $m/n \sim 1/1$, where m and n stand for the

toroidal and poloidal mode numbers, respectively, propagating in the ion-diamagnetic direction. The amplitude of TAE at the Mirnov coil position is evaluated to be on the order of 10^{-5} T for this shot. The experimentally observed mode frequency is consistent with the TAE gap frequency f_{TAE} represented by $f_{TAE} = v_A / 4\pi R q^*$ ($q^* = (2m+1)/2n$).

A TAE eigenfunction for the discharge shown in Fig. 2 was found by the AE3D code [16] in the experimentally observed frequency range. Figure 3 shows shear Alfvén continua calculated by the STELLGAP code [17] and the TAE eigenfunction at the frequency of 69.8 kHz, respectively, in addition to profiles of T_e , n_e and rotational transform $\iota/2\pi$ used in this analysis. The MHD equilibrium was reconstructed by the VMEC2000 code in the free boundary condition. Subsequently, the eigenfunction was computed for $n=1$ and $m=0\sim 10$. As can be seen in Fig. 3d), the eigenfunction of the experimentally observed TAE is composed of two dominant Fourier components. The figure also indicates that the TAE observed in the discharge shown in Fig. 2 has an odd parity, having the peak of the eigenfunction at the normalized minor radius r/a of ~ 0.6 . It is interesting to note that, unlike observation in tokamaks, the odd TAE is often strongly destabilized in LHD in comparison with the even TAE.

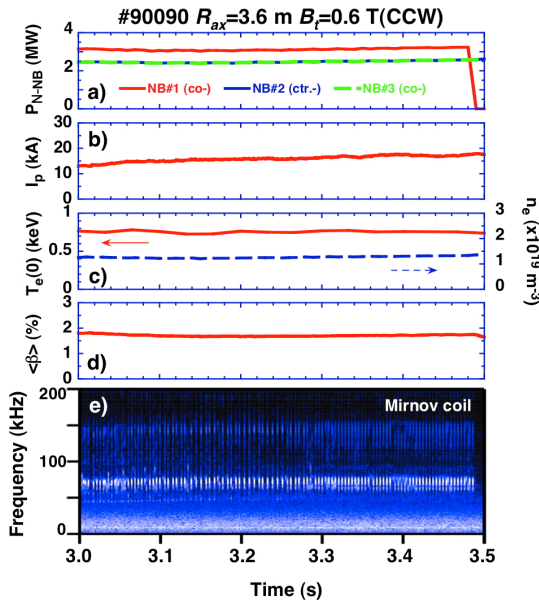


FIG. 2. Typical waveforms of TAE discharge in LHD at R_{ax}/B_t of 3.6 m/0.6 T(CCW). a) Absorbed power of tangential N-NBs. b) Co-flowing net current dominated by Ohkawa current. c) Central electron temperature $T_e(0)$ and line-averaged electron density. d) Volume-averaged beta value. e) Magnetic spectrogram.

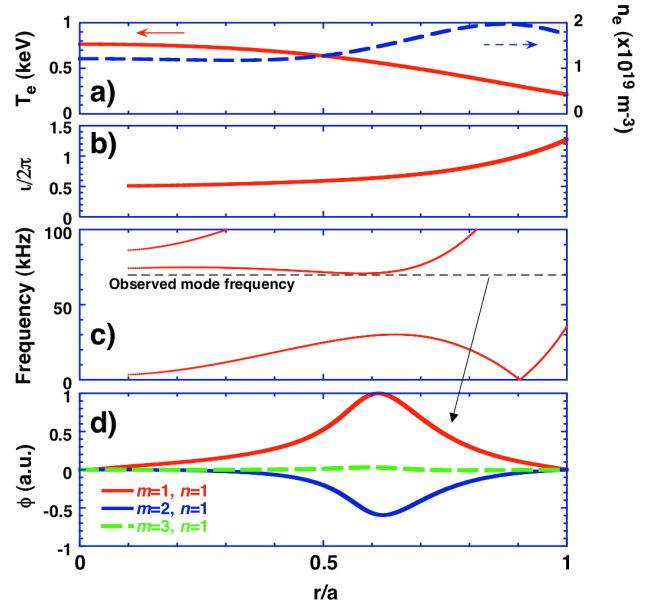


FIG. 3. a) Profiles of T_e , n_e for the discharge shown in Fig. 2. b) Rotational transform profile. c) Shear Alfvén continua calculated by the STELLGAP code. Experimentally observed mode frequency is also shown by a broken line. d) TAE eigenfunction calculated by the AE3D code at $f = 69.8$ kHz.

3.2 TAE-induced energetic ion transport and loss

In LHD, anomalous radial transport of co-going beam ions toward the outboard side of the torus caused by TAEs has been recognized from rapid increases in CX fast neutrals measured

with E//B-type NPA having a tangential line of sight [11]. The SLIP placed at the outboard side contributes to a deeper understanding of the anomalous behavior of energetic beam ions while TAEs are destabilized. Figure 4 shows time traces of a) amplitude of magnetic fluctuations δB_{TAE} filtered in the TAE frequency range, b) CX-fast neutral flux ($E=154.3$ keV) and c) energetic-ion loss rate to SLIP $\Gamma_{SLIP\#9}$. The subscript “SLIP#9” corresponds to a specific PMT viewing a specific position on the scintillator screen. Actually, $\Gamma_{SLIP\#9}$ corresponds to $E \sim E_b$ and $\chi \sim 40$ degrees at the SLIP position, as shown later in Figure 8. As can be seen in Fig. 4b), correlated with each TAE burst, recurrent increases of fast neutral flux originating from co-going beam ions are observed at the energy of ~ 150 keV. Significant increases in $\Gamma_{SLIP\#9}$ due to TAE bursts are also observed. This indicates that a substantial transport/loss of co-going energetic beam ions toward the outboard side is induced by $m/n \sim 1/1$ TAEs in R_{ax}/B_t of 3.6 m/0.6 T.

Figure 5 shows the dependence of the increment of $\Gamma_{SLIP\#10}$ normalized by the parameter of beam pressure, i.e. the product of P_{N-NB} and τ_{se} due to TAEs in $E \sim 100$ keV and $\chi \sim 40$ degrees at the SLIP position. Here, τ_{se} is the Spitzer’s slowing down time on electron. $\delta\Gamma_{SLIP\#10}$ is evaluated with the difference in the beam-ion loss rate between the value of the pulse peak and that right before each TAE burst. As seen in other devices [8, 10, 18], $\delta\Gamma_{SLIP}$ increases as $\delta B_{TAE}/B_t$ increases. It appears that the increment of $\delta\Gamma_{SLIP}$ has a quadratic dependence on $\delta B_{TAE}/B_t$ in this discharge. According to Ref. 19, a diffusive-type loss process is suggested. Note that the tendency of $\delta\Gamma_{SLIP}$ vs. $\delta B_{TAE}/B_t$ is configuration-dependent. In an outward-shifted configuration with R_{ax} of 3.9 m, $\delta\Gamma_{SLIP}$ increases much more steeply as $\delta B_{TAE}/B_t$ increases. It should also be noted that the TAE-induced beam-ion loss is not very significant in higher B_t discharges, since $\delta B_{TAE}/B_t$ becomes smaller and the deviation of transit energetic-ion orbits from magnetic flux surfaces tends to be smaller as B_t increases.

It is interesting to note that high-frequency fluctuations in Γ_{SLIP} correlated with the TAE frequency were observed using a correlation analysis between Γ_{SLIP} and Mirnov coil signal, as seen from the spectrogram of coherence in Fig. 6c). In this shot, the deposition power of N-NBs P_{N-NB} increases at $t=2.8$ s due to the increase in electron density by gas puffing. As seen

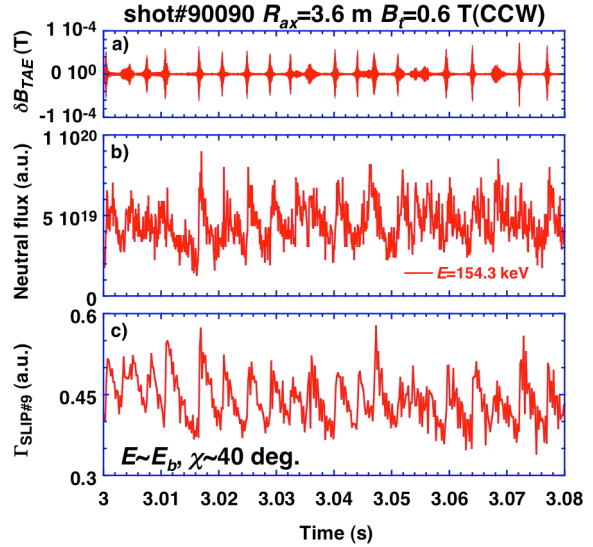


FIG. 4. Time traces of a) magnetic fluctuation amplitude of TAEs at the Mirnov coil position, b) charge-exchanged fast-neutral flux ($E=154.3$ keV), and c) energetic-ion loss rate to SLIP ($E \sim E_b$, $\chi \sim 40$ degrees).

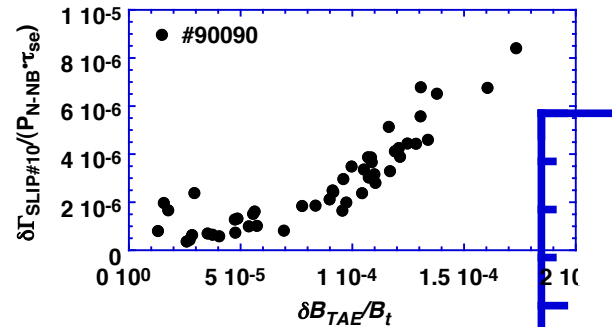


FIG. 5. Energetic-ion loss rate to SLIP as a function of $\delta B_{TAE}/B_t$ at the Mirnov coil position. τ_{se} is the Spitzer’s slowing down time on electron.

in Fig. 6b), the significant rise of $\Gamma_{SLIP\#5}$ for energetic ions with $E \sim E_b$ and $\chi \sim 50$ degrees at the SLIP position is observed, resulting from the increase of P_{N-NB} . The Lorentz orbit code using a vacuum magnetic field suggests that energetic ions having transitional orbits in the co-going phase are responsible for making the $\Gamma_{SLIP\#5}$ spot. After the increase in P_{N-NB} , $\Gamma_{SLIP\#5}$ fluctuating in the same frequency as TAEs is clearly recognized. This indicates that energetic beam ions detected by the SLIP are those that interacted strongly with TAEs. Because the SLIP can detect energetic ions having co-going transit orbits or transitional orbits in the co-going phase, this observation suggests that tangentially co-injected energetic ions are responsible for the TAE excitation in this discharge. High-frequency beam-ion loss fluxes correlated with the TAE are also observed in the domain of low energy ($E \sim 20$ keV) and low pitch angle ($\chi \sim 30$ degrees) [20]. The ratio of the velocity of these slowed down beam ions having passing orbits to v_A is evaluated to be about 0.4 and satisfies the sideband excitation condition for TAE ($v_{\parallel}/v_A = 1/3$) [21]. The high-frequency fluctuations in Γ_{SLIP} therefore suggest that fundamental and sideband excitations of TAEs coexist due to energetic beam ions.

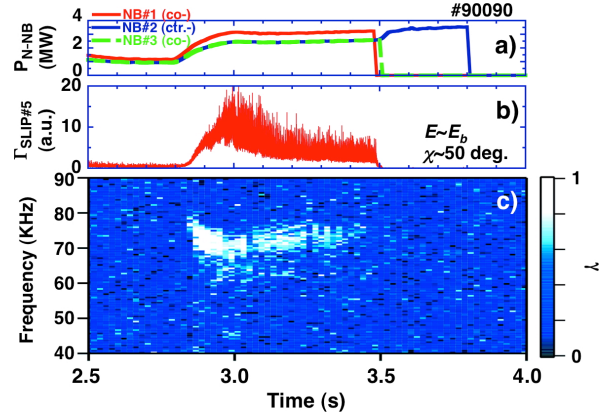


FIG. 6. a) Time traces of deposition power of three N-NBs. b) Energetic ion loss rate to SLIP. Energy and pitch angle are ~ 180 keV and ~ 50 degrees, respectively, at the SLIP position. c) Spectrogram of coherence γ between energetic-ion loss rate to SLIP and Mirnov coil signal.

4. Analyses of the effects of perturbed magnetic field on energetic-ion transport

To increase our understanding of experimentally observed beam ion losses due to TAEs, we simulated beam ion orbits considering possible amplitudes of magnetic fluctuations. The calculation scheme is as follows. After the MHD equilibrium is reconstructed using experimental data by the VMEC2000 code, the deposition of beam ions is calculated by the HFREYA code [22]. Subsequently, the deposition data are fed into the DELTA5D code [23] and guiding center orbits of beam ions are computed on the Boozer coordinates. The magnetic fluctuation is represented through $\delta\mathbf{B} = \nabla \times \alpha\mathbf{B}$, where α is a general function of the position,

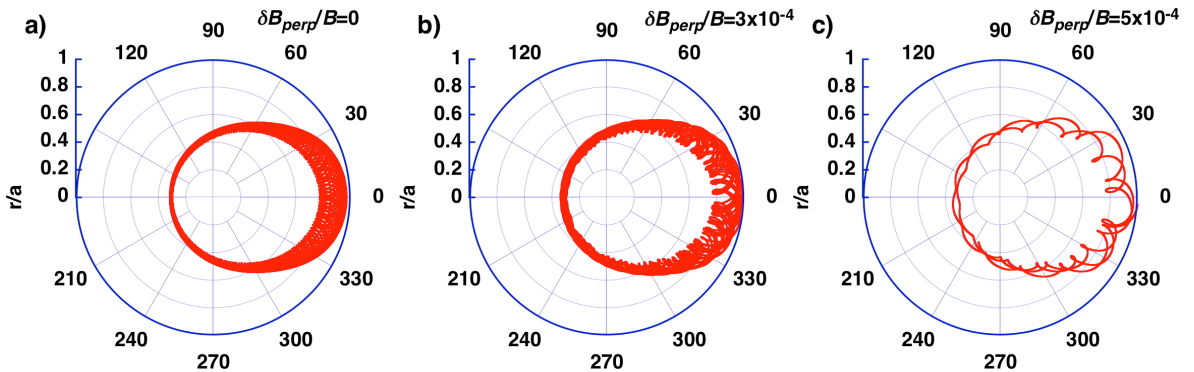


FIG. 7. Effect of perturbed magnetic field on co-going beam ion orbit in LHD at R_{ax}/B_t of 3.6 m/0.6 T. Energy and initial pitch angle of beam ions are 180 keV and 15 degrees, respectively.

amplitude and frequency of the magnetic fluctuation. As for the profile of α , the internal structure of TAE ($m/n \sim 1/1$) predicted by the AE3D code is used. For simplicity, the amplitude and frequency of the mode are fixed, not time-dependent, in this analysis. Figure 7 shows orbits of co-going transit beam ions having E of 180 keV and initial χ of 15 degrees for three different amplitudes of magnetic fluctuation. The model calculation indicates that orbits of co-going beam ions tend to expand toward the outboard side of the torus as the amplitude of magnetic fluctuation increases. This result qualitatively supports the experimentally observed anomalous transport and/or loss of co-going beam ions due to the MHD instabilities.

Figure 8 shows experimentally obtained two-dimensional distribution of scintillation light on the scintillator screen measured with an image-intensified fast CMOS camera due to the impact of escaping beam ions in the discharge shown in Fig. 4. ρ_h vs. χ map and viewing positions of 16 PMTs are overlaid on this screen. Three primary spots can be recognized in $(\rho_h(\text{cm}), \chi(\text{deg.})) = (10 \sim 15, 28 \sim 35)$, $(8 \sim 18, 35 \sim 45)$ and $(8 \sim 18, 45 \sim 55)$. The brightest spot peaks at a relatively high pitch-angle region, i.e., $\chi \sim 52$ degrees, and its energy at the peak is somewhat lower than E_b , i.e. $E \sim 150$ keV ($\rho_h \sim 15$ cm). This spot always exists even in a phase without TAEs and is attributed to strikes of escaping beam ions that experience collisional ripple transport. Actually, the Lorentz orbit calculation suggests that this brightest spot is caused by energetic ions having transitional orbits in the co-going phase. Two other, weaker spots in the lower χ ranges are attributable to co-going transit ions whose orbits deviate largely from magnetic flux surfaces. The effect of TAEs on the brightest spot exists but is not very significant. $\Delta I_{SLIP\#6}/I_{SLIP\#6}$ is about +10%. Stronger effects of TAE on the energetic-ions loss rate can be seen in the lower χ range of less than 45 degrees or in the high-energy range, e.g. $I_{SLIP\#9}$ shown in Fig. 4c), $I_{SLIP\#10}$ shown in Fig. 5) and $I_{SLIP\#5}$ shown in Fig. 6).

Next, efforts to compare between experimental and simulation data have been made in order to study beam-ion loss signals seen on the scintillator screen. To do this, first we calculate spatial, energy and pitch-angle distributions of escaping beam ions at the last closed flux surface (LCFS) by the DELTA5D code. The resulting information about energetic ion losses at the LCFS is fed into the Lorentz orbit code as an initial condition. Orbits of

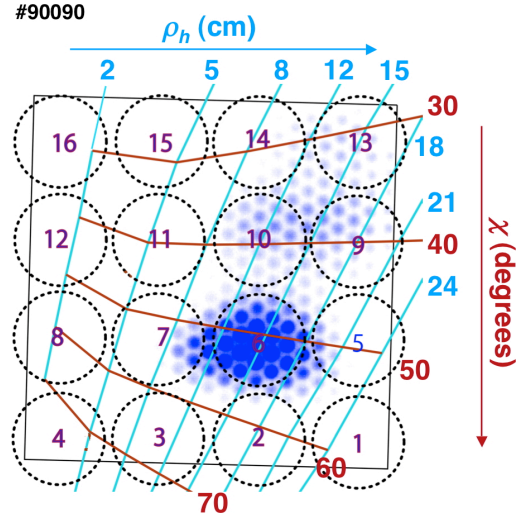


FIG. 8. Distribution of scintillation light due to impact of escaping energetic ions on the scintillator screen in the shot#90090.

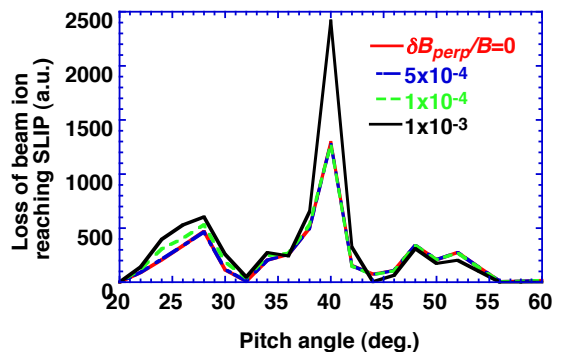


FIG. 9. Pitch-angle distributions of escaping energetic ions reaching the SLIP for four different amplitudes of magnetic fluctuations. Collisions between energetic ions and background plasma are taken into account.

energetic ions lunched from the LCFS are tracked in a vacuum magnetic field, and then ions reaching the SLIP are picked up. We use this scheme because the DELTA5D code uses the equilibrium data calculated by VMEC2000 and is therefore applicable only to the inside of LCFS. Orbit calculations are carried out with four different possible amplitudes of magnetic fluctuations. Calculated pitch-angle distributions of escaping energetic ions reaching the SLIP are shown in Fig. 9. Here, the number of particles is integrated over energy because the SLIP energy resolution is poorer than that of pitch-angle resolution. As seen in Fig. 9, the orbit simulation reproduces the experimental observation for the χ distribution. The calculation also suggests that, as expected, beam-ion loss increases as $\delta B_{perp}/B$ increases. The effects of magnetic fluctuations on beam-ion losses are more visible in the lower range of χ (<45 degrees) compared with the beam ion loss in $\chi \sim 50$ degrees. This feature is consistent with that of the experimental observation mentioned above. However, there is a discrepancy in that the beam-ion loss rate near $\chi \sim 50$ degrees is strongest in the measurement, whereas in the present simulation it is not the strongest. Further efforts are required to resolve the discrepancy between the two results for intensity distribution in χ of lost energetic ions at the SLIP.

6. Summary

Experimental results on TAE-induced anomalous transport of tangentially injected energetic beam ions and consequent beam-ion losses in LHD are presented. The results showed that $m/n \sim 1/1$ TAE instabilities driven by co-going beam ions lead to significant beam ion transport and losses toward the outboard side of the torus. The energetic-ion loss rate was significantly enhanced as the amplitude of TAE fluctuation increased. It has an approximately quadratic dependence on the fluctuation amplitude. Escaping energetic ion fluxes fluctuating with the frequency of TAEs were found to interact strongly with TAEs. High-frequency fluctuation components of beam-ion loss flux were clearly observed in the energy range of co-going transit orbits where the resonance conditions of the fundamental and sideband excitation of TAE are satisfied. The pitch-angle distributions of escaping ions reaching the SLIP were reproduced by particle simulation considering ripple structure, collisions with background plasma and a perturbed magnetic field having the TAE frequency. Significant effects of TAEs on energetic-ion losses were experimentally seen, especially in the low-pitch-angle region. The modeled particle calculation also supported the increment in beam-ion loss due to magnetic fluctuation in the low-pitch-angle region.

Acknowledgements

This work was supported in part by the LHD project budget (NIFS08ULHH101) and in part by Grands-in-Aid for Scientific Research (B) from the Japan Society for the Promotion of Science, Nos. 21340175 and 21360457. This work was also supported by Japan/U.S. Cooperation in Fusion Research and Development. The authors are grateful to the LHD operation group for their excellent technical support.

References

- [1] CHEN, C.Z. and CHANCE, M.S., "Low- n shear Alfvén spectra in axisymmetric toroidal plasmas", *Phys. Fluids* **29** (1986) 3695.
- [2] CHEN, L., "Theory of magnetohydrodynamic instabilities excited by energetic particles in tokamaks", *Phys. Plasmas* **1** (1994) 1519.

- [3] WONG, K.L., et al., “Excitation of toroidal Alfvén eigenmodes in TFTR”, Phys. Rev. Lett. **66** (1991) 1874.
- [4] FASOLI, A., et al., “Chapter 5: Physics of energetic ions”, Nucl. Fusion **47** (2007) S264.
- [5] WELLER, A., et al., “Neutral beam driven global Alfvén eigenmodes in the Wendelstein W7-AS stellarator”, Phys. Rev. Lett. **72** (1994) 1220.
- [6] TOI, K., et al., “MHD modes destabilized by energetic ions on LHD”, Fus. Sci. Technol. **58** (2010) 186.
- [7] DARROW, D.S., et al., “MHD induced neutral beam ion loss from NSTX plasmas”, Nucl. Fusion **48** (2008) 084004.
- [8] GARCÍA-MUÑOZ, M., et al., “Fast-ion losses induced by ACs and TAEs in the ASDEX Upgrade tokamak”, Nucl. Fusion **50** (2010) 084004.
- [9] ZHU, Y.B., et al., “Phenomenology of energetic-ion loss from the DIII-D tokamak”, Nucl. Fusion **50** (2010) 084024.
- [10] ISOBE, M., et al., “Studies of fast-ion transport induced by energetic particle modes using fast-particle diagnostics with high time resolution in CHS”, Nucl. Fusion **46** (2006) S918.
- [11] OSAKABE, M., et al., “Experimental observations of enhanced radial transport of energetic particles with Alfvén eigenmode on the LHD”, Nucl. Fusion **46** (2006) S911.
- [12] KOMORI, A., et al., “Goal and achievements of Large Helical Device project”, Fus. Sci. Technol. **58** (2010) 1.
- [13] TAKEIRI, Y., et al., “High performance of neutral beam injectors for extension of LHD operational regime”, Fus. Sci. Technol. **58** (2010) 482.
- [14] ISOBE, M., et al., “Fast-particle diagnostics on LHD”, Fus. Sci. Technol. **58** (2010) 426.
- [15] OGAWA, K., et al., “Installation of bidirectional lost fast-ion probe in the Large Helical Device”, J. Plasma Fusion Res. SERIES **8** (2009) 655.
- [16] SPONG, D.A., et al., “Clustered frequency analysis of shear Alfvén modes in stellarators”, Phys. Plasmas **17** (2010) 022106.
- [17] SPONG, D.A., et al., “Shear Alfvén continua in stellarators”, Phys. Plasmas **10** (2003) 3217.
- [18] FREDRICKSON, E.D., et al., “Collective fast ion instability-induced losses in National Spherical Tokamak Experiment”, Phys. Plasmas **13** (2006) 056109.
- [19] HEIDBRINK, W.W., et al., “The nonlinear saturation of beam-driven instabilities : theory and experiment”, Phys. Fluids **B5** (1993) 2176.
- [20] OGAWA, K., et al., “Observation of energetic-ion losses induced by various MHD instabilities in the Large Helical Device”, Nucl. Fusion **50** (2010) 084005.
- [21] BIGLARI, H., et al., “On resonant destabilization of toroidal Alfvén eigenmodes by circulating and trapped energetic ions/alpha particles in tokamaks”, Phys. Fluids **B4** (1992) 2385.
- [22] MURAKAMI, S., et al., “Finite β effects on the ICRF and NBI heating in the Large Helical Device”, Trans. Fusion Technol. **27** (1995) 256.
- [23] SPONG, D.A., et al., “NCSX plasma heating methods”, Fus. Sci. Technol. **51** (2007) 203.